Korean J. Chem. Eng.
DOI: 10.1007/s11814-022-1293-y

pISSN: 0256-1115
eISSN: 1975-7220

Low generational cystamine core PAMAM derivatives modified with nuclear localization signal derived from lactoferrin as a gene carrier

Jeil Lee*, Yong-Eun Kwon, Hwanuk Guim***, and Kyung Jae Jeong*,†**

*Department of Chemical Engineering, University of New Hampshire, Durham, New Hampshire 03824, United States
**Center for Scientific Instrumentation, Korea Basic Science Institute, 169-148 Gwahak-ro, Yuseong-gu, Daejeon 34133, Korea
***Research Center for Materials Analysis, Korea Basic Science Institute, 169-148 Gwahak-ro, Yuseong-gu, Daejeon 34133, Korea

(*Received 15 July 2022 • Revised 13 September 2022 • Accepted 15 September 2022*)

Abstract−Polyamidoamine (PAMAM) dendrimer has received much attention as an alternative to polyethylenimine (PEI) for gene delivery due to the relatively low cytotoxicity. In general, low generational PAMAM dendrimers have better biocompatibility than high generational dendrimers but suffer reduced transfection efficiency. Transfection efficiency can be improved by the modification of the polymer with nuclear localization signal (NLS) peptides. In this study, we modified low generational cystamine core PAMAM dendrimers (cPAMAM, generation 0, 1 and 2) with a lactoferrin-derived nuclear localization signal (NLS) peptide and evaluated transfection efficiency and cytotoxicity as a function of the number of conjugated NLS peptides using NIH 3T3, MCF-7 and human dermal fibroblasts (HDFs). The transfection efficiency of NLS-modified cPAMAM G2 was the highest among the cPAMAM derivatives and similar or higher than PEI 25 kDa. The cytotoxicity of cPAMAM derivatives was generation-dependent and significantly lower than PEI 25 kDa. Our study indicates that cPAMAM G2 conjugated with NLS is a promising candidate for gene delivery applications.

Keywords: Nonviral Vector, Cationic Polymer, Polyamidoamine (PAMAM) Dendrimer, Transfection, Nuclear Localization Signal (NLS)

INTRODUCTION

Gene therapy, a method of delivering genes to the cells to correct genetic disorders, requires a carrier called a vector [1,2]. Initially, recombinant viruses were used as a vector because of their excellent transduction and targeting capacity. Since Glybera was approved by the European Union (EU) as the first gene medicine in 2012, the development of viral vectors for gene therapy has accelerated. In the United States (US), Imlygic was approved as the first gene medicine and many viral vectors were approved by the Food and Drug Administration (FDA) since [1]. However, viral vectors require co-transfection of various plasmid DNA, and its complex process and low yields lead to high production costs. Moreover, several health risks, such as multiple organ failure induced by high immunogenicity, carcinogenesis and oncogene activation by point mutagenesis, and the potential pathogenicity remain as major challenges [3,4].

Nonviral vectors were developed as an alternative to viral vectors. Despite the ease of chemical modification, production, and quality control, and reduced cytotoxicity, immunogenicity, and manufacturing costs than viral vectors, the low selectivity and transfection efficiency of nonviral vectors limit their applications in gene therapy [2,5]. However, recent progress in mRNA vaccines have demonstrated the feasibility of using nonviral gene vectors for clinical applications [6].

Nonviral vectors can be classified into cationic polymers, cationic lipids, and inorganic nanoparticles. They form complexes with negatively charged DNA molecules by electrostatic interaction; the complex of cationic polymer with DNA is called 'polyplex' [7]. Although PEI has been the most widely used cationic polymer for gene delivery, its excessive positive charges induce cytotoxicity, and it is non-biodegradable. Other biodegradable alternatives such as cationic polyamino acids, chitosan, poly(2-dimethylaminoethyl methacrylate) (PDMAEMA), and polyamidoamine (PAMAM) dendrimer that consists of biodegradable linkers suffer from the low transfection efficiency compared to PEI [8-12].

One major challenge to improve transfection efficiency of nonviral vectors is to increase the accumulation of polyplexes near the nuclear region after endocytosis [13]. Conjugation of cationic polymers with nuclear localization signal (NLS) sequences has been proposed to mitigate that challenge and been shown to increase transfection efficiency [14-17]. NLS sequences are short peptides consisting of positively charged amino acids, recognized by various cargo proteins in the cytoplasm for the nuclear transport [18].

When dendrimer is used as a cationic polymer for gene delivery, the generation number - the number of interior layers consisting of repeating units radially attached to the core - is another important factor [19]. In general, as the generation number increases, the transfection efficiency is improved but with increased cytotoxicity.

Cytotoxicity of polyplexes is known to be caused by two differ-

†To whom correspondence should be addressed.
E-mail: KyungJae.Jeong@unh.edu

ent mechanisms [20]. The polycations that were not internalized can induce apoptosis by binding to and damaging the cell membranes. The internalized polycations can also damage the mitochondrial membranes, generating hydroxyl radicals and activating multiple apoptotic pathways [21]. As the generation number increases, the tendency of polyplexes to disrupt cell membranes and mitochondria also increases due to the increased positive charges. Therefore, the generation of NLS-modified PAMAM dendrimers should be carefully controlled [22,23].

In this study, we conjugated a lactoferrin protein-derived NLS sequence, GRRRR [24,25], to cystamine core PAMAM dendrimers (cPAMAM) of low generations (G0, G1 and G2) to find the optimal formulation for improved transfection efficiency and reduced cytotoxicity of the polyplexes. A histidine residue was added to the original NLS sequence to further lower the cytotoxicity of PAMAM derivatives [26,27]. Histidine, one of the essential amino acids, is a natural antioxidant that is capable of scavenging hydroxyl radicals by its imidazole group [28]. In previous study, a histidine residue was added to the original NLS sequence to further lower the cytotoxicity of PAMAM derivatives. Therefore, we synthesized cPAMAM derivative with modified histidine and NLS sequence.

EXPERIMENTAL SECTION

1. Materials

Starburst® Poly(amidoamine) (PAMAM) dendrimer, Generation 0, 1, and 2 - Cystamine Core - Amine Surface were purchased from Andrews ChemServices (Berrien Springs, MI, USA). Polyethylenimine (branched, 25 kDa), heparin sodium salt from porcine intestinal mucosa, N,N-dimethylformamide (DMF), dimethylsulfoxide (DMSO), N,N-diisopropylethylamine (DIPEA), Dithiotreitol (DTT) piperidine, triisopropylsilane (TIS), and trifluoroaceticacid (TFA), were purchased from Sigma-Aldrich (Burlington, MA, USA). N-Hydroxybenzotriazole (HOBt), 2-(1H-benzotriazole-1-yl)-1,1,3,3-tetra-methyluronium (HBTU), Fmoc-Gly-OH, Fmoc-His(trt)-OH, and Fmoc-Arg(pbf)-OH were obtained from Anaspec (San Jose, CA, USA). Luciferase Assay System and Reporter Lysis 5x Buffer were bought from Promega (Madison, WI, USA). Alexa 546 Nucleic Acid Labeling Kit, TrypLETM Express, AlamarBlue, Quant-iT^{TM} PicoGreen^{TM} dsDNA Reagent, Micro BCA Protein Assay Kit, Fetal bovine serum (FBS), Dulbecco's phosphate-buffered saline (DPBS), Dulbecco's modified eagle's medium (DMEM), 100X antibiotic-antimycotic reagent were obtained from Thermo Fisher Scientific (Waltham, MA, USA). The Micro BCA Protein Assay Kit was purchased from Pierce (Rockford, IL, USA).

2. Synthesis of Cystamine Core PAMAM Derivatives Conjugated with GRRRR Sequence

10 mg of cPAMAM G0 (cPG0), cPAMAM G1 (cPG1), and cPAMAM G2 (cPG2) was dissolved in methanol, dried by nitrogen gas, and lyophilized. The lyophilized cPAMAM dendrimers were dissolved in 1.5 mL of an anhydrous mixture of N,N-dimethylformamide (DMF)/dimethyl sulfoxide (DMSO) (2 : 1, v/v) and mixed with four eq. of Fmoc-His(trt)-OH, HOBt, and HBTU and eight eq. of DIPEA. The equivalence of added coupling reagents and amino acids was calculated based on the number of amine groups containing each dendrimer. The mixture solution was prepared in a total volume of 2.5 mL DMF/DMSO (4 : 1, v/v) and stirred at 37 °C for 18 h. Fmoc-His(trt)-grafted dendrimers were precipitated and washed by cold diethyl ether. The precipitation and washing steps were performed at 2,200 rpm for 3 min to eliminate diethyl ether and repeated three times. The washed dendrimers were dried with nitrogen gas, dissolved, and stirred in a 2 mL piperidine solution (30 : 70, piperidine/DMF, v/v) for Fmoc deprotection at 37 °C for 2 h in the dark. The deprotected His(trt)-grafted dendrimers were precipitated, washed, and dried as mentioned above. The deprotected His(trt)-grafted dendrimers were dissolved in anhydrous DMF and mixed with Fmoc-Arg(pbf)-OH and coupling reagents. The conjugation of additional amino acids and Fmoc deprotection steps was performed for GRRRRH-cPAMAM derivatives as mentioned above. The deprotection of trt and pbf protection groups was performed at 25 °C for 8 h in a mixture solution (95 : 2.5 : 2.5, trifluoroacetic acid/triisopropylsilane/distilled water, v/v/v) after conjugation of all amino acids. Deprotected cPAMAM derivatives were precipitated, washed, and dried, as mentioned above. The synthesized cPAMAM derivatives were dissolved in distilled water. In the light of each cPAMAM derivative, synthesized GRRRRH-cPG0, GRRRRH-cPG1, and GRRRRH-cPG2 were placed in tubing (Spectra/Por, molecular weight cut-off of 1,000, 3,500, and 10,000, respectively). GRRRRH-cPG0, GRRRRH-cPG1, and GRRRRH-cPG2 were dialyzed in distilled water for 18 h and were obtained as white powders after lyophilization.

3. Plasmid DNA Preparation

The luciferase expression plasmid DNA (pCN-Luci) that subcloned the Photinus pyralis luciferase cDNA and NLS derived from SV40 large T antigen was made as reported previously [16]. The pCN-Luci was transformed into *E. coli* TOP10 competent cells and cultured. The extraction of pCN-Luci from *E. coli* cells was performed using the NucleoBond Xtra Midi Plus kit (Macherey-Nagel, Dueren, Germany). The eluted pCN-Luci was precipitated and washed twice by 2-propanol. Finally, pCN-Luci was dried by nitrogen gas, resuspended in distilled water, and stored at −20 °C.

4. Picogreen Assay for Characterization of DNA Complexation and Release

cPG0, cPG1, cPG2, GRRRRH-cPG0, GRRRRH-cPG1, and GRRRRH-cPG2 were prepared at 1 mg/mL, mixed with pCN-Luci (0.5 μg) for complexation, and incubated for 30 min. The respective polymer/pCN-Luci polyplexes were prepared at weight ratios ranging from 0.5 : 1 to 16 : 1. The HEPES buffer (25 mM, pH 7.4) was added to polyplexes, and mixtures were prepared in a total volume of 200 μL. Then, 200 μL of 0.5% PicoGreen solution (0.5 : 99.5, PicoGreen reagent/TE buffer) was mixed with each polyplex solution and the respective mixtures (20 μL) were placed in 96-well plates. Finally, 80 μL of TE buffer (10 mM Tris, 1 mM EDTA, pH 7.5) was added per well and complexation between polymer and DNA was evaluated using fluorescence intensity measured by Synergy H1^{TM} Hybrid Multi-Mode Microplate Reader (BioTek Instrument, Inc., Winooski, VT, USA). The excitation and emission wavelengths were 490 and 520 nm, respectively. DNA release tests were performed to verify polyplex disruption by DTT and heparin. Each polyplex was prepared at a weight ratio of 2 : 1 as mentioned above, and DTT and heparin were treated to polyplexes at concentrations ranging from 0 to 40 mM and μg/mL, respectively. Then, each polyplex

was incubated for 30 min. The release of DNA was measured as described above.

5. Acid-Base Titration Assay

The buffing capacity of cPAMAM derivatives was measured by acid-base titration, and PEI 25 kDa, cPG0, cPG1, and cPG2 were used as controls. The respective polymers (1.04×10^{-7} mol) were added to the mixture solution (4 mL of 150 mM NaCl and 1 N NaOH (100 μL) and prepared in a total volume of 5 mL. Each polymer solution was titrated with 40 μL aliquots of 0.1 N hydrogen chloride (HCl) until the pH reached 3. Titration experiments were performed using a Fisher Science Education™ Laboratory Benchtop pH Meters (Thermo Fisher Scientific, Waltham, MA, USA).

6. Diameter and ζ-Potential Measurements of Polyplexes

To make polyplexes, pCN-Luci (2 μg) and polymers were mixed and incubated for 30 min. The polyplexes were prepared at weight ratios from 0.5 : 1 to 12 : 1. Then they were diluted by distilled water in a total volume of 1.6 mL. The diameter and ζ-potentials were measured at 25 °C using Zeta-potential & Particle Size Analyzer ZetaPALS (Brookhaven Instruments, Holtsville, NY, USA).

7. Scanning Transmission Electron Microscopy (-in-SEM) Imaging and Low-voltage Energy Dispersive X-ray Spectroscopy (EDS) Analysis

All polyplexes were prepared in a total volume of 10 μL at a weight ratio of 12 : 1. The respective polyplexes were added to ethanol and prepared in a total volume of 800 μL in ethanol (75 : 25, ethanol/water, v/v). Each polyplex (2 μL) was placed on the 200-mesh ultrathin carbon-supported copper grids and dried at 60 °C for 16 h. The images of polyplexes were measured using field emission scanning electron microscope (FE-SEM, Merlin Compact, Carl Zeiss Inc., Oberkochen, Germany) in dark-field image mode at 30 kV. EDS analysis (XFlash 6160, Bruker; takeoff angle: 35°; detector area 60 mm^3) of observed polyplexes was performed under the condition of 10 kV in consideration of maximum cross-section of the ionization of phosphorus for optimized analysis. The working distance (WD) and analysis time were 8.3 mm and 100 s, respectively.

8. Cell Culture

NIH3T3 mouse embryonic fibroblast cells, MCF-7 human breast cancer cells, and human dermal fibroblast cells (HDFs) were cultured in the growth medium (89 : 10 : 1, DMEM/FBS/antibiotic-antimycotic reagent, v/v/v). All cell culture was performed using Nunc EasYFlask 75 cm^2 (Thermo Fisher Scientific, Portsmouth, NH, USA) at 37 °C in a humidified atmosphere (5% CO_2/95% air, v/v).

9. Transfection Assay

NIH3T3 and MCF-7 cells were cultured in 96-well plates at a density of 1.8×10^4 cells/well and HDFs were prepared in 96-well plates at a density of 1.3×10^4 cells/well. Cells were incubated for 16 h to obtain 70-80% confluency. Polyplexes were formed in a total volume of 30 μL in growth medium by mixing pCN-Luci (0.5 μg) with PEI 25 kDa, cPG0, cPG1, cPG2, GRRRRH-cPG0, GRRRRH-cPG1, and GRRRRH-cPG2 for 30 min. The polymer : DNA weight ratio was 1 : 1 for PEI 25 kDa, 16 : 1 for cPG0, cPG1, and cPG2, and 4 : 1-16 : 1 for GRRRRH-cPG0, GRRRRH-cPG1 and GRRRRH-cPG2. The weight ratios for PEI 25 kDa, cPG0, cPG1, and cPG2 were chosen for the optimal transfection efficiency based on our previous results. The polyplexes were added to cells and were incubated for 24 hours. Then the cells were washed with 100 μL of Dulbecco's phosphate-buffered saline (DPBS) per well, and 80 μL of reporter lysis buffer as diluted 1 mg/mL concentration was added to each well. 96-well plates were then placed in a shaker at 150 rpm for 30 min at room temperature. The lysed cells were moved to microtubes and centrifuged at 13,200 rpm for 10 min and cell lysates were transferred to new microtubes. Subsequently, 10 μL of each lysate and 20 μL luciferin were mixed in a 96-well low volume white plate (PerkinElmer, Boston, MA, USA). The luciferase activity of lysates was measured using Centro XS3 LB 960 (Berthold Technology, Bad Wildbad, Germany), and the protein concentration in each lysate was measured using a Micro BCA™ protein assay kit. Finally, the transfection efficiency of each cPAMAM derivative was calculated in terms of a relative light unit (RLU) per microgram of total protein.

10. Cytotoxicity Assay

Cytotoxicity of the polymers was evaluated using the alamarBlue reagent. MCF-7 and NIH3T3 cells were cultured in 96-well plates at a density of 1.8×10^4 cells/well and HDFs were prepared in 96-well plates at a density of 1.3×10^4 cells/well for 16 h to reach 70%-80% confluency before the addition of polymers. The polymers at various concentrations (10-160 μg/mL) were added to the cells, and cells were incubated for 24 h at 37 °C. Then, 10 μL alarmarBlue reagent was added per well and incubated for 2 h at 37 °C. The excitation and emission wavelengths of each plate were measured at 560 and 590 nm, respectively (BioTek Instrument, Inc., Winooski, VT, USA).

11. Preparation of Alexa Fluor 546-labeled pCN-Luci and Confocal Microscopy

The labeling of pCN-Luci using Alexa Fluor 546 was performed as described in the manufacturer's protocol. The NIH3T3 cells were cultured at a density of 1.5×10^4 cells/well in Thermo Scientific™ Nunc glass-bottom dishes. cPG0, cPG1, cPG2, GRRRRH-cPG0, GRRRRH-cPG1, GRRRRH-cPG2, and PEI 25 kDa/pCN-Luci polyplexes were prepared at the polymer : DNA weight ratios that resulted in the optimal transfection efficiency. 24 h after the incubation, cells were washed by Dulbecco's phosphate-buffered saline (DPBS). To stain the nuclei, the cells were treated with 20 μg/mL DAPI for 15 min. After washing with DPBS, the cells were fixed with 4% paraformaldehyde. Finally, the cells were washed by DPBS again and cellular images were obtained using a Nikon A1R Laser scanning confocal fluorescence microscope.

12. Statistical Analysis

Statistical analysis was performed using GraphPad Prism 5 software, and the significant differences were analyzed using one-way analysis of variance (ANOVA) with Tukey's multiple comparison test: *P<0.05, **P<0.01, and ***P<0.001.

RESULTS AND DISCUSSION

1. Synthesis and Characterization of cPAMAM Derivatives Conjugated with the GRRRRH Sequence

Generally, PAMAM modified with NLS sequences shows relatively increased cytotoxicity compared with that of native PAMAM because NLS sequences consist of cationic amino acids; however, when the histidine residues and NLS sequences are simultaneously introduced to PAMAM dendrimer, the cytotoxicity is reduced with-

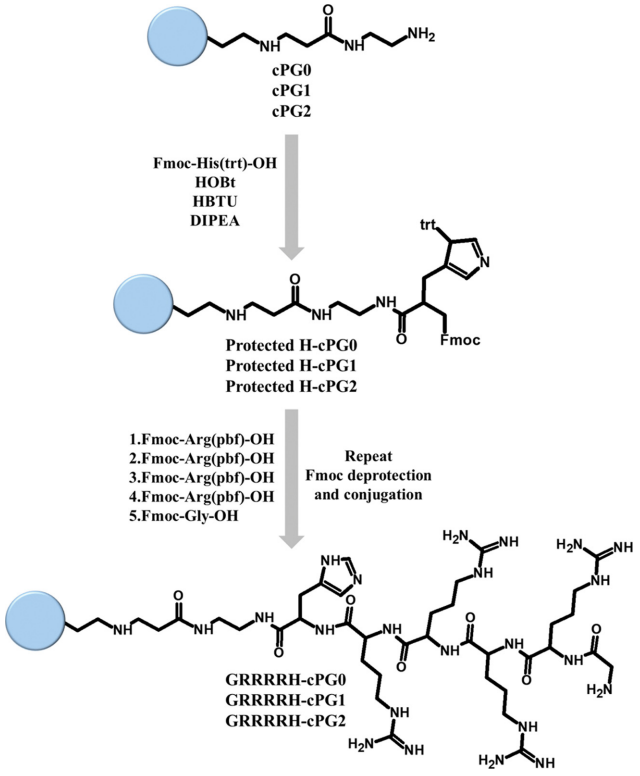

Scheme 1. Synthesis scheme of cPAMAM derivatives conjugated with nuclear localization signal.

out altering the transfection efficiency [27].

In this study, we added the GRRRRH sequence to the amine groups of cPAMAM of generations 0 - 2 (designated as cPG0, cPG1 and cPG2, respectively) by HOBt and HBTU coupling reactions to find an optimal gene carrier (Scheme 1). The relative conjugation yield and molecular weight of cPAMAM derivatives modified with GRRRRH sequence were analyzed using H NMR spectroscopy (Fig. 1 and Table 1). The final conjugation yields of GRRRRH-cPG0, GRRRRH-cPG1, and GRRRRH-cPG2 were 30%, 99%, and 82%, respectively (Table S1). The peak assignments are as follows.

GRRRRH-cPG0: δ (in ppm) 1.58 (-CHCH$_2$C**H$_2$**CH$_2$NH- of arginine), 1.72 (-CHC**H$_2$**CH$_2$CH$_2$NH- of arginine), 2.59 (-NCH$_2$C**H$_2$**CO- of cPAMAM), 2.93 (-SCH$_2$C**H$_2$**N- of cPAMAM), 3.13 (-CHCH$_2$C**H$_2$**NH- of arginine, -HCC**H$_2$**CCHNCHNH- of histidine, -NC**H$_2$**CH$_2$CO- of cPAMAM, and -SC**H$_2$**CH$_2$N- of cPAMAM), 3.19 (-NC**H$_2$**CH$_2$CO- of cPAMAM, -CHCH$_2$CH$_2$C**H$_2$**NH- of arginine), 3.20 (-CONHC**H$_2$**CH$_2$NHCO- of cPAMAM), 3.26 (-CONHCH$_2$C**H$_2$**NHCO- of cPAMAM), 3.82 (-NHCOC**H$_2$**NH$_2$- of glycine), 4.03 (-**H**CCH$_2$CH$_2$CH$_2$NH- of arginine), 4.19 (-**H**CCH$_2$CH$_2$CH$_2$NH- of arginine), 4.23 (-**H**CCH$_2$CH$_2$CH$_2$NH- of arginine) 4.28 (-**H**CCH$_2$CH$_2$CH$_2$NH- of arginine), 4.51 (-**H**CCH$_2$CCHNCHNH- of histidine), 7.12 (-HCCH$_2$CC**H**NCHNH- of histidine) and 8.18 (-HCCH$_2$CCHNC**H**NH- of histidine). **GRRRRH-cPG1**: δ (in ppm) 1.57 (-CHCH$_2$C**H$_2$**CH$_2$NH- of arginine), 1.74 (-CHC**H$_2$**CH$_2$CH$_2$NH- of arginine), 2.56 (-NCH$_2$C**H$_2$**CO- of cPAMAM), 3.13 (-CHCH$_2$CH$_2$C**H$_2$**NH- of arginine, -HCC**H$_2$**CCHNCHNH- of histidine, -NC**H$_2$**CH$_2$CO- of cPAMAM, -SC**H$_2$**CH$_2$N- of cPAMAM, -SCH$_2$C**H$_2$**N- of cPAMAM, and -CONHCH$_2$C**H$_2$**N- of cPAMAM), 3.19 (-CONHC**H$_2$**CH$_2$NHCO- of cPAMAM), 3.28 (-CONHC**H$_2$**CH$_2$NHCO- of cPAMAM), 3.41 (-CONHCH$_2$C**H$_2$**NHCO- of cPAMAM), 3.82 (-NHCOC**H$_2$**NH$_2$- of glycine), 4.19 (-**H**CCH$_2$CH$_2$CH$_2$NH- of arginine), 4.24 (-**H**CCH$_2$CH$_2$CH$_2$NH- of arginine), 4.28 (-**H**CCH$_2$CH$_2$CH$_2$NH- of arginine), 4.51 (-**H**CCH$_2$CCHNCHNH- of histidine), 7.11 (-HCCH$_2$CC**H**NCHNH- of histidine) and 8.15 (-HCCH$_2$CCHNC**H**NH- of histidine). **GRRRRH-cPG2**: δ (in ppm) 1.57 (-CHCH$_2$C**H$_2$**CH$_2$NH- of arginine), 1.73 (-CHC**H$_2$**CH$_2$CH$_2$NH- of arginine), 2.51 (-NCH$_2$C**H$_2$**CO- of cPAMAM), 2.89 (-CONHCH$_2$C**H$_2$**N- of cPAMAM), 3.12 (-CHCH$_2$CH$_2$C**H$_2$**NH- of arginine, -HCC**H$_2$**CCHNCHNH- of histidine, -NC**H$_2$**CH$_2$CO- of cPAMAM, -SC**H$_2$**CH$_2$N- of cPAMAM, and -SCH$_2$C**H$_2$**N- of cPAMAM), 3.17 (-CONHC**H$_2$**CH$_2$NHCO- of cPAMAM), 3.27 (-CONHC**H$_2$**CH$_2$NHCO- of cPAMAM), 3.36 (-CONHCH$_2$C**H$_2$**NHCO- of cPAMAM), 3.81 (-NHCOC**H$_2$**NH$_2$- of glycine), 4.18 (-**H**CCH$_2$CH$_2$CH$_2$NH- of arginine), 4.23 (-**H**CCH$_2$CH$_2$CH$_2$NH- of arginine), 4.28 (-**H**CCH$_2$CH$_2$CH$_2$NH- of arginine), 4.49 (-**H**CCH$_2$CCHNCHNH- of histidine), 7.05 (-HCCH$_2$CC**H**NCHNH- of histidine) and 8.04 (-HCCH$_2$CCHNC**H**NH- of histidine).

2. Complexation and Decomplexation Analysis of cPAMAM Derivatives Conjugated with the GRRRRH Sequence

Naked plasmid DNA has limited cellular uptake due to the large hydrodynamic diameter (~μm) and electrostatic repulsion with the cellular membrane because of its negative charges. Complexation with cationic polymers can condense plasmid DNA into nanosized

Table 1. Relative molecular weight calculated by ^{1}H NMR and charge numbers

Sample	MW (Da)	No. of +charge/polymer	No. of +charge/μg[c]
cPG0	609[a]	4	4.0×10^{15}
cPG1	1,522[a]	8	3.2×10^{15}
cPG2	3,348[a]	16	2.9×10^{15}
GRRRRH-cPG0	3,653[b]	20	3.3×10^{15}
GRRRRH-cPG1	8,092[b]	40	3.0×10^{15}
GRRRRH-cPG2	14,618[b]	72	3.0×10^{15}

[a]Molecular weight is provided by the manufacturer.
[b]Molecular weight is calculated by ^{1}H NMR of each polymer.
[c]The N/P ratio of each polyplex at 1 : 1 weight ratio (polymer:DNA) is 2.2 for cPG0, 1.7 for cPG1, 1.6 for cPG2, 1.8 for GRRRRH-cPG0, 1.6 for GRRRRH-cPG1, and 1.6 for GRRRRH-cPG2.

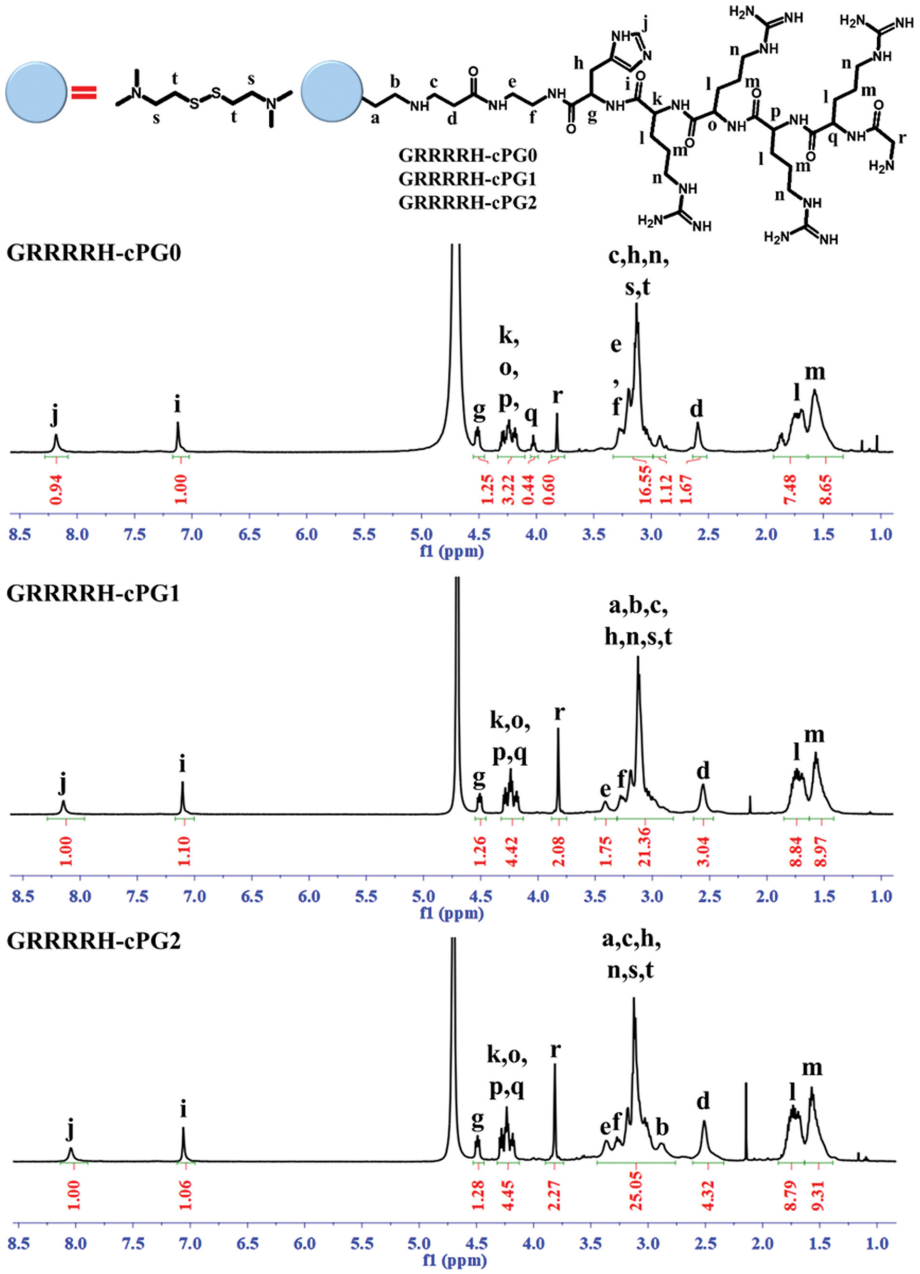

Fig. 1. ^{1}H NMR spectra of cPAMAM derivatives. S and t are used instead of a and b in GRRRRH-cPG0.

particles with net positive charges and help plasmid DNA to be internalized into the cytoplasm by electrostatic interactions with the cellular membrane [29].

To confirm weight ratios of PAMAM polymer and plasmid DNA (pCN-Luci) that form stable polyplexes, we performed the PicoGreen exclusion assay (Fig. 2). This assay operates by enhanced fluorescence of the reagent as it intercalates in the DNA base pairs. When plasmid DNA and polymers form stable complexes, the intercalation of PicoGreen reagent in the DNA base pairs is hindered, resulting in reduced fluorescence [30].

For most polymers, both modified or unmodified, stable polyplexes were beginning to form at a weight ratio of 2 : 1 (polymer : DNA) evidenced by the near zero fluorescence (Fig. 2(a)). The only exception was cPG0, which formed the stable polyplex with the DNA at a weight ratio of 8 : 1.

Next, we studied the disruption of polyplexes in the presence of heparin, an anionic polymer, and DTT, a reductant. This study is relevant to the PAMAM-based gene delivery because it emulates the gradual DNA release from the polyplexes by competitive interactions with anions and anionic moieties of various proteins once the polyplexes escape from the endosomes or the cleavage of the disulfide bond of cPAMAM core by reductants such as glutathione.

The polyplexes of NLS-conjugated cPAMAM dendrimers were in general more stable than the unmodified dendrimers in the presence of heparin and DTT (Fig. 2(b) and 2(c)). This can be attributed to the increased electrostatic attraction due to the increased number

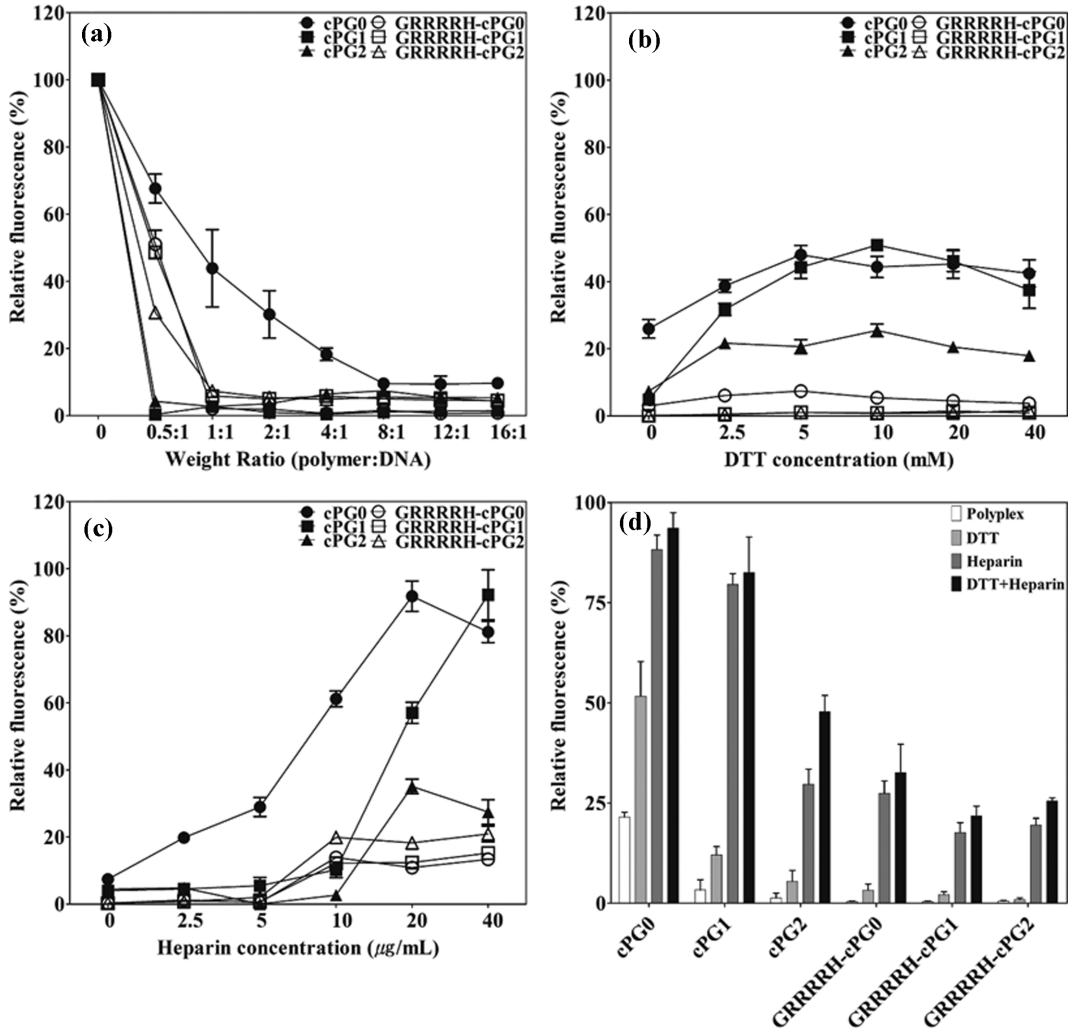

Fig. 2. (a) Complexation analysis of pCN-Luci with cPAMAM derivatives using PicoGreen reagent at various weight ratios. (b) Analysis of polyplex disruption induced by reductants. (c) Analysis of polyplex disruption induced by polyanions. (d) Evaluation of polyplex disruption induced by reductants and polyanions (with 40 mM DTT and 40 μg/mL heparin). Data are shown as mean±standard deviation (n=3).

of amine groups on the NLS-conjugated cPAMAM (by ~5 fold). When the polyplexes were treated with both heparin and DTT (with 40 mM DTT and 40 μg/mL heparin), the disruption of polyplexes was further enhanced (Fig. 2(d)). These results point to the possibility that the presence of anionic molecules and reductants in the cytoplasm will assist in the release of DNA once the polyplexes escape from the endosomes [31].

3. Proton Buffering Capacity and Physical Properties Evaluation of cPAMAM Derivatives Conjugated with the GRRRRH Sequence

Proton buffering capacity of cationic polymers is a good indicator of successful gene delivery. Cationic polymers, once they are internalized by endocytosis, absorb protons, causing osmotic imbalance between endosome and cytosol, leading to endosome disruption and the release of DNA into the nuclear region [13,31,32]. Fig. 3 shows the result of acid-base titration experiment to evaluate the proton buffering capacity of cPAMAM derivatives.

cPAMAM derivatives conjugated with NLS sequences showed

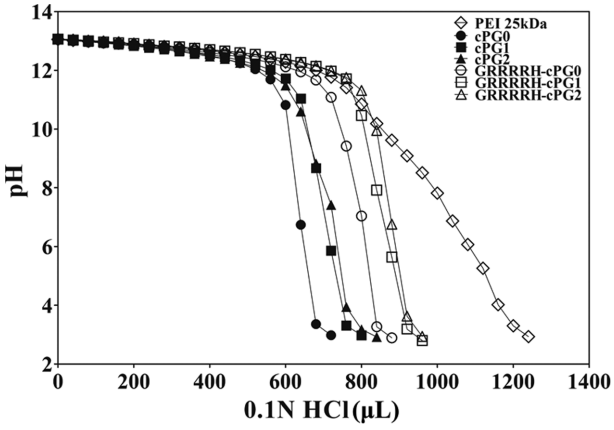

Fig. 3. Acid-base titration profiles of the polymers.

increased buffering capacity compared to that of native cPAMAM dendrimers due to the abundant guanidinium groups from the argi-

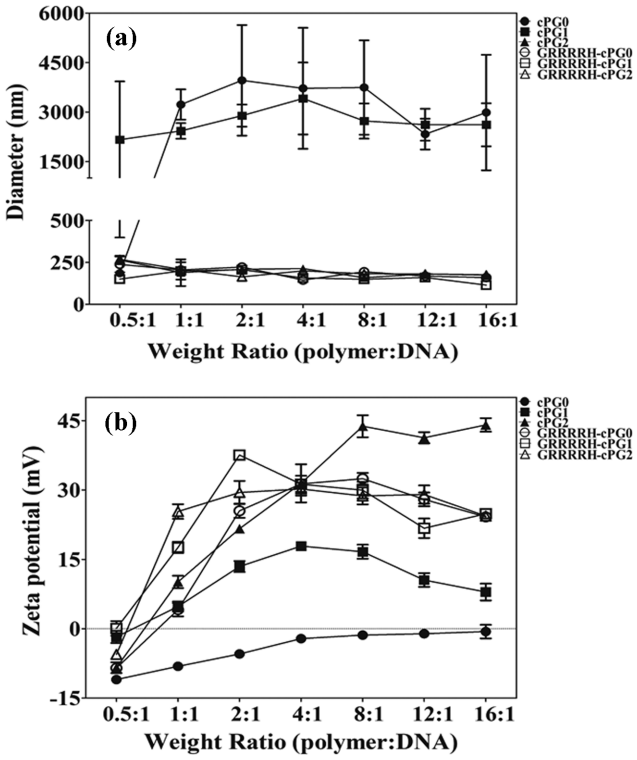

Fig. 4. (a) Size and (b) ζ-potential analysis of cPAMAM derivatives/pCN-Luci polyplexes. Data are shown as mean±standard deviation (n=3).

nine residues. The improved buffering capacity indicates the potential for improved transfection efficiency. However, all cPAMAM derivatives showed lower proton buffering capacity than PEI 25 kDa, as PEI contains more primary amines per molecule.

Next, we studied the effects of polymer : DNA weight ratios on the size and ζ-potential of polyplexes (Fig. 4). cPG0 and cPG1 formed micro-sized polyplexes with plasmid DNA and low net charges at all weight ratios, whereas cPG2 and NLS-conjugated cPAMAM derivatives formed nanoparticles (<300 nm) and suitable positive charges. Although cPG0 and cPG1 had weight ratios that indicated stable complexation, their diameters were insufficient for internalization by endocytosis. cPG0 and cPG1 have amine groups <10, whereas cPG2 and cPAMAM derivatives conjugated with NLS peptides have amine groups >16. Considering the size and ζ-potential of each polyplex, these results imply that cationic polymers must possess over 16 amine groups to form the nano-sized polyplexes for gene delivery.

Scanning transmission electron microscopy (STEM) was used to visualize the polyplexes and confirm the size measurements from the dynamic light scattering (DLS) method (Fig. 5). The observed polyplexes showed an oval or spherical shape. Although the polyplexes were polydisperse in size, the average size of polyplexes was consistent with the DLS analysis. Energy-dispersive X-ray spectroscopy (EDS) was performed to analyze atomic composition of the nanoparticles. Phosphorus, an intrinsic element of DNA and carbon, nitrogen and oxygen were detected from the nanoparticles, indicating that the nanoparticles were polyplexes formed between NLS-conjugated cPAMAM and DNA. Other peaks such as aluminum, silicon, copper, and sulfur originated from the sample stage, EDS detector, TEM grid, and buffer solution of DNA extraction kit, respectively.

4. Transfection Efficiency of cPAMAM Derivatives Conjugated with the GRRRRH Sequence

Transfection efficiency of cPAMAM derivatives was studied using the plasmid for luciferase with varying polymer : DNA ratios (4 : 1-16 : 1 (w/w)) based on the characterization of polyplex formation (Fig. 2). Two widely used cell lines (NIH 3T3 and MCF-7) and a primary cell type, human dermal fibroblasts (HDFs) were used for the study (Fig. 6 and Fig. S2).

Addition of the NLS sequence to cPAMAM increased transfection efficiency by one to three orders of magnitude for all cPAMAM generations. The benefit of adding the NLS sequence is the clearest for the case of cPG2, because the addition of the NLS sequence did not alter the size of polyplexes but resulted in two orders of magnitude higher transfection efficiency [32,33]. Among the cPAMAM derivatives, GRRRRH-cPG2 showed higher transfection efficiency than PEI in NIH 3T3 cells (at polymer : DNA ratio higher than 12 : 1) and similar transfection efficiency in HDFs [31,34].

Transfection efficiency of the cPAMAM derivatives was also influenced by polymer : DNA ratio. In general, transfection efficiency increased as polymer : DNA ratio increased even when the size of the polyplexes did not change significantly. This can be explained by the increase in non-complexed cPAMAM derivatives. In gene delivery using cationic polymers, the role of free polymers that do not form polyplexes with DNA is important. Although the detailed mechanism by which free polymers affect transfection requires further study, it is generally believed to be due to the interaction between free polymers and cell membranes. The free polymers would intercalate in cellular and endosomal membranes electrostatically and make nanosized holes. The membranous barriers weakened by free polymers enhance cellular uptake of polyplexes and endosomal escape, resulting in improved transfection efficiency. As expected, the transfection efficiency was much lower for the primary cells (HDFs) than for two other cell lines.

Although the exact mechanism for much improved transfection efficiency of the cPAMAM derivatives compared with those of native cPAMAM dendrimers requires a further study, it can be attributed to the following three factors. The first is the formation of more stable and smaller polyplexes with DNA due to the increased charge density. Compared with cPG2, cPG0 and cPG1 formed unstable and micro-sized large polyplexes, which explains the improved transfection efficiency by about 10-fold in NIH 3T3 and MCF-7 cells. Conjugation with the NLS sequence further increases positive charges, resulting in more improved transfection efficiency.

The second is the improved cellular uptake resulting from the guanidinium groups of the NLS sequence. Guanidinium groups, existing on arginine residues, can form electrostatic bonds and hydrogen bonds simultaneously with phospholipids on cell membranes [35,36]. The presence of guanidium groups at the right ratios with primary amines are known to improve the penetration of polyplexes into the cytoplasm compared to the polyplexes that contain only primary amines [37-39]. Lysine can also have a positive charge, but its effect on transfection efficiency of PAMAM-based vectors was

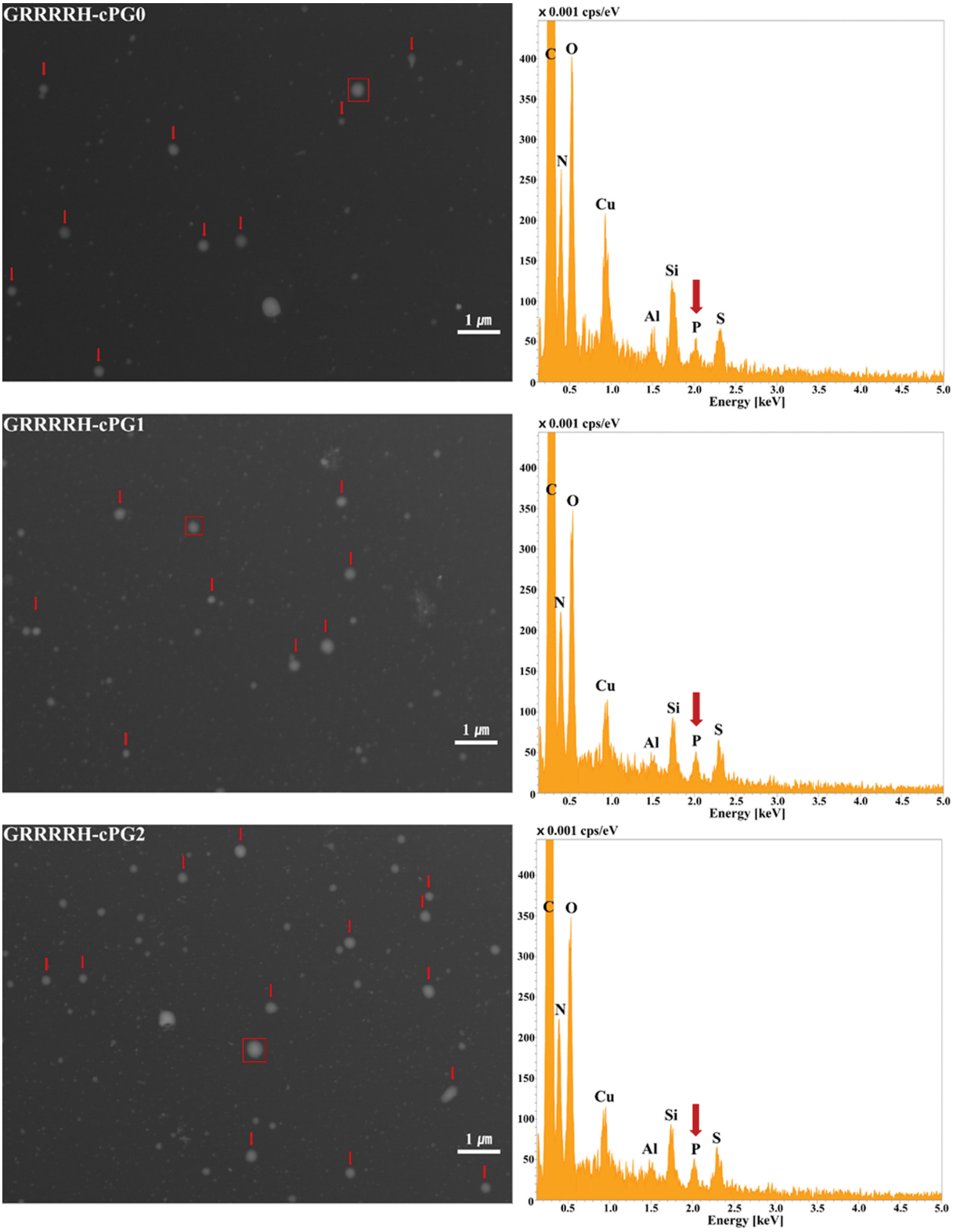

Fig. 5. STEM (-in-SEM) images and EDS analysis of polyplexes.

shown to be lower than that of arginine [40].

The last factor is the enhanced accumulation of polyplexes near the nucleus due to the NLS sequence. The NLS is a signal sequence that is recognized by cargo proteins and can facilitate the transport of large biological molecules into the nucleus. NLS sequences of PAMAM derivatives are recognized by various cargo proteins in the cytoplasm, which enables the transport of polyplexes to the proximity of nucleus [41]. This increases the chance of their transport

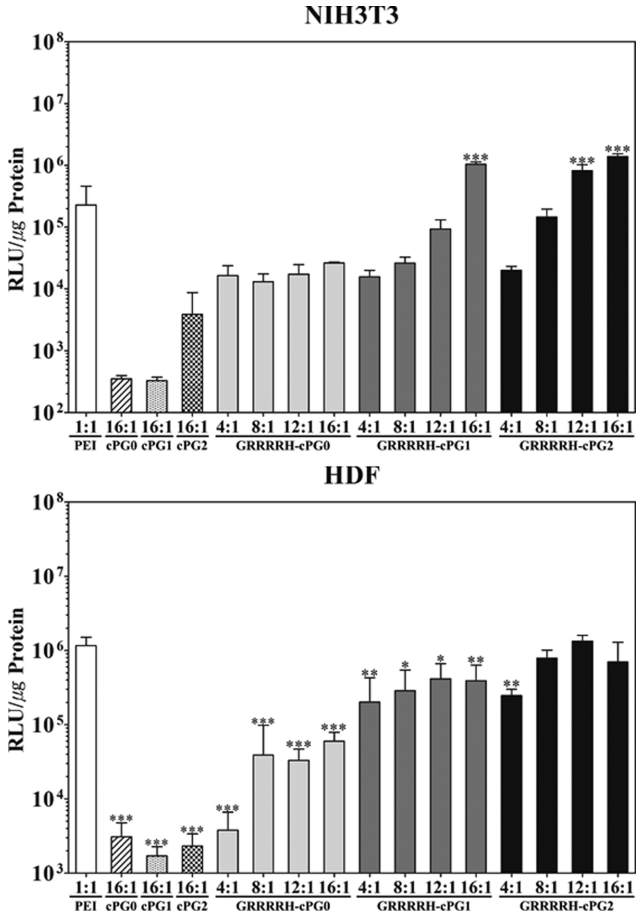

Fig. 6. Transfection efficiency of cPAMAM derivatives in NIH3T3 and HDF cells. Data are shown as mean±standard deviation (n=3). *p<0.05, **p<0.01, and ***p<0.001 compared to PEI.

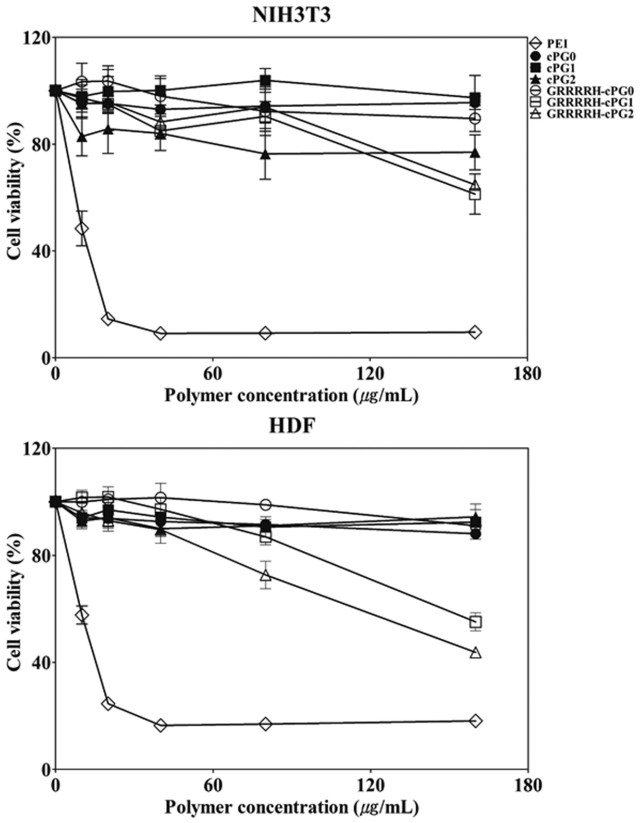

Fig. 7. Cytotoxicity assay in NIH 3T3 cells and HDFs using alarmarBlue assay. Data are shown as mean±standard deviation (n=3).

into the nuclear region when the nuclear envelope disappears during mitosis [31,34].

5. Cytotoxicity Evaluation of cPAMAM Derivatives Conjugated with the GRRRRH Sequence

Cytotoxicity of cPAMAM derivatives was measured by the alamarBlue assay (Fig. 7 and Fig. S3). Overall, cPAMAM dendrimers exhibited much less cytotoxicity than PEI. GRRRRH-cPG1 and GRRRRH-cPG2 showed considerable cytotoxicity only at high polymer concentration (>80 μg/mL). An increase in positive charges of cationic polymers improves the polyplex formation and transfection efficiency, but is known to increase cytotoxicity by disrupting cellular and mitochondrial membranes, leading to apoptosis by the generation of reactive oxygen species (ROS) [20,22,42]. Considering these factors altogether, GRRRRH-cPG2 is an ideal vector as it achieves comparable transfection efficiency as PEI with much lower cytotoxicity when used at concentrations lower than 80 μg/mL.

6. Intracellular Distribution of cPAMAM Derivatives/pCN-Luci Polyplexes

Based on the physical properties and transfection efficiency of cPAMAM derivatives, we conclude that the enhanced transfection efficiency might be associated with the accumulation of polyplex near the nuclear region induced by the NLS sequence, which is consistent with the previous studies. To verify this hypothesis, we visualized the intracellular distribution of cPAMAM derivatives/pCN-Luci polyplexes in NIH 3T3 cells using confocal microscopy (Fig. 8 and Fig. S4). To distinguish between the nuclear DNA and plasmid DNA, the plasmid DNA was pre-labeled with a different fluorophore.

cPAMAM derivatives conjugated with the NLS sequence/pCN-Luci polyplexes were predominantly distributed around the nuclear region compared with those of native cPAMAM dendrimers/pCN-Luci polyplexes. The level of accumulation of plasmid DNA near the nuclei was consistent with the transfection efficiency (Fig. 8).

CONCLUSION

We conjugated GRRRR sequence, an NLS derived from the lactoferrin protein to cPAMAM dendrimers, and demonstrated that the introduction of the NLS sequence increased transfection efficiency of cPAMAM dendrimers by several orders of magnitude for both cell lines and primary cells. Transfection efficiency and cytotoxicity were dependent on the cPAMAM generation. Compared to PEI, all cPAMAM derivatives showed much less cytotoxicity than PEI, while the transfection efficiency of GRRRRH-cPG2 was similar or higher than PEI 25 kDa. Our results indicate that GRRRRH-cPG2 has the potential as an effective and safe gene carrier for various gene therapies.

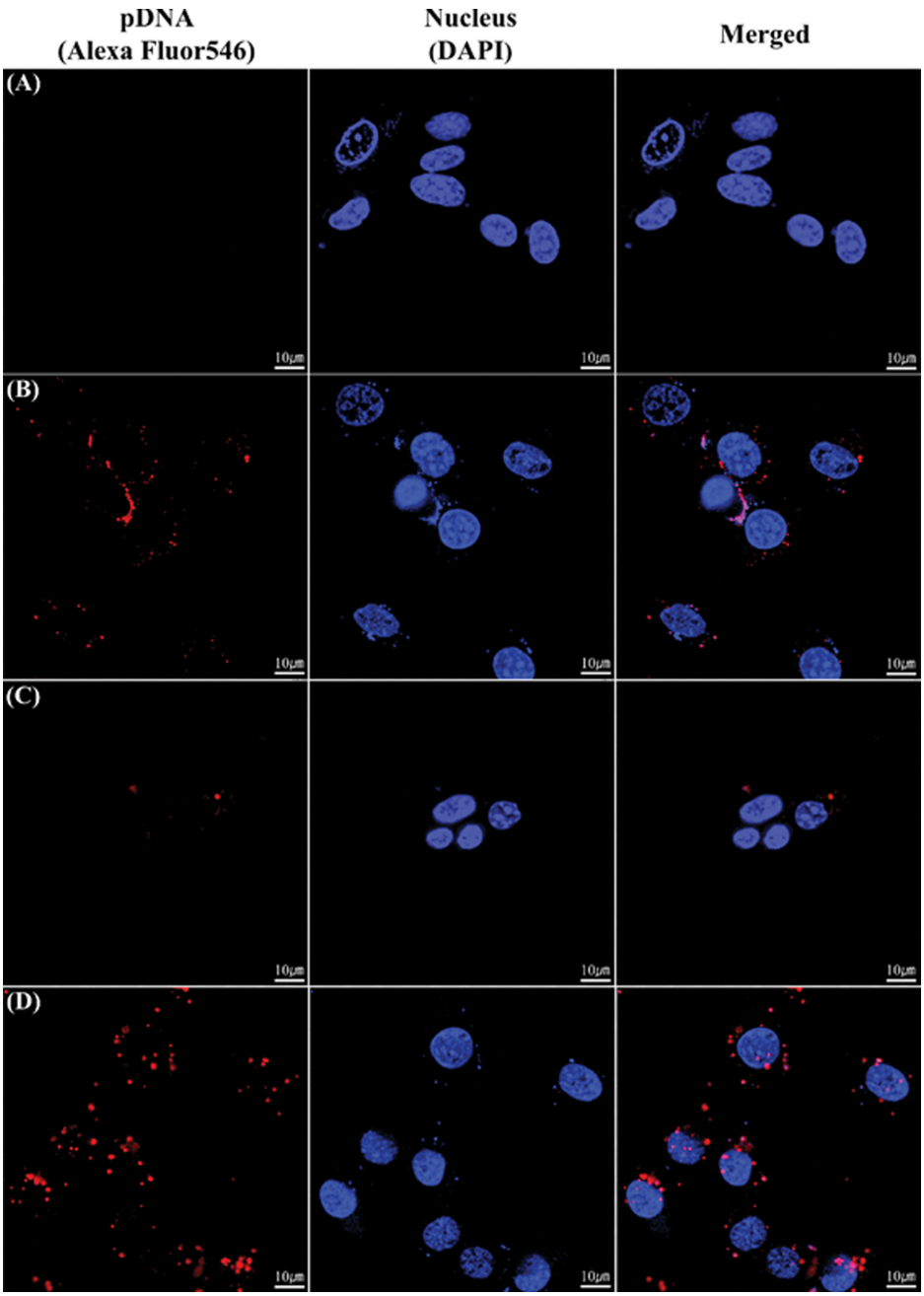

Fig. 8. Confocal microscope images of polyplexes of (a) Cells only, (b) PEI, (c) cPG2, (d) GRRRRH-cPG2 with pCN-Luci in NIH3T3 cells. PEI, native cPAMAM dendrimers, and cPAMAM derivatives conjugated with the NLS sequence/pCN-Luci polyplexes were prepared at 1 : 1 and 16 : 1 and treated to NIH3T3 cells.

ACKNOWLEDGEMENT

This research was sponsored by the U.S. National Science Foundation and was accomplished under the Grant No. OIA-1757371.

SUPPORTING INFORMATION

Additional information as noted in the text. This information is available via the Internet at http://www.springer.com/chemistry/journal/11814.

REFERENCES

1. M. R. Cring and V. C. Sheffield, *Gene Ther.*, **29**, 3 (2020).
2. M. Ramamoorth and A. Narvekar, *J. Clin. Diagn.*, **9**(1), GE01 (2015).
3. Y. Wang, K. F. Bruggeman, S. Franks, V. Gautam, S. I. Hodgetts, A. R. Harvey, R. J. Williams and D. R. Nisbet. *Adv. Healthc. Mater.*, **10**(1), 2001238 (2021).
4. E. Ayuso, *Mol. Ther. Methods Clin. Dev.*, **3**, 15049 (2016).
5. P. Wu, H. Chen, R. Jin, T. Weng, J. K. Ho, C. You, L. Zhang, X. Wang and C. Han, *J. Transl. Med.*, **16**(1), 1 (2018).

6. C. Rinoldi, S. Zargarian, S. P. Nakielski, X. Li, A. Liguori, F. Petronella, D. Presutti, Q. Wang, M. Costantini and L. De Sio, *Small Method.*, **5**(9), 2100402 (2021).
7. L. Zhu and R. I. Mahato, *Expert Opin. Drug Deliv.*, **7**(10), 1209 (2010).
8. Y. Cheng, R. C. Yumul and S. H. Pun, *Angew. Chem. Int. Ed.*, **55**(39), 12013 (2016).
9. Y. S. Lee and S. W. Kim, *J. Control. Release*, ***190***, 424 (2014).
10. Y. Liu, J. Li, K. Shao, R. Huang, L. Ye, J. Lou and C. Jiang, *Biomaterials*, **31**(19), 5246 (2010).
11. T. H. Kim, J. E. Ihm, Y. J. Choi, J. W. Nah and C. S. Cho, *J. Control. Release*, **93**(3), 389 (2003).
12. J. M. Benns, J.-S. Choi, R. I. Mahato, J.-S. Park and S. W. Kim, *Bioconjug. Chem.*, **11**(5), 637 (2000).
13. U. Lächelt and E. Wagner, *Chem. Rev.*, **115**(19), 11043 (2015).
14. J. Lee, J. Jung, Y.-J. Kim, E. Lee and J. S. Choi, *Int. J. Pharm.*, **459**(1-2), 10 (2014).
15. K. Ma, M. X. Hu, Y. Qi, J. H. Zou, L. Y. Qiu, Y. Jin, X.-Y. Ying and H. Y. Sun, *Biomaterials*, **30**(30), 6109 (2009).
16. Y. M. Bae, H. Choi, S. Lee, S. H. Kang, Y. T. Kim, K. Nam, J. S. Park, M. Lee and J. S. Choi, *Bioconjug. Chem.*, **18**(6), 2029 (2007).
17. J. S. Choi, K. S. Ko, J. S. Park, Y. H. Kim, S. W. Kim and M. Lee, *Int. J. Pharm.*, **320**(1-2), 171 (2006).
18. T. Boulikas, *Crit. Rev. Eukaryot. Gene Expr.*, **3**(3), 193 (1993).
19. N. T. Pourianazar, P. Mutlu and U. Gunduz, *J. Nanoparticle Res.*, **16**(4), 1 (2014).
20. S. M. Moghimi, P. Symonds, J. C. Murray, A. C. Hunter, G. Debska and A. Szewczyk, *Mol. Ther.*, **11**(6), 990 (2005).
21. X. Li, S. Hao, A. Han, Y. Yang, G. Fang, J. Liu and S. Wang, *J. Mater. Chem. B*, **7**(25), 4008 (2019).
22. R. Jevprasesphant, J. Penny, R. Jalal, D. Attwood, N. B. McKeown and A. D'emanuele, *Int. J. Pharm.*, **252**(1-2), 263 (2003).
23. J. Haensler and F. C. Szoka Jr., *Bioconjug. Chem.*, **4**(5), 372 (1993).
24. S. Kumari and A. K. Kondapi, *Int. J. Biol. Macromol.*, **108**, 401 (2018).
25. S. Penco, S. Scarfi, M. Giovine, G. Damonte, E. Millo, B. Villaggio, M. Passalacqua, M. Pozzolini, C. Garrè and U. Benatti, *Biotechnol. Appl. Biochem.*, **34**(3), 151 (2001).
26. J. Lee, S. Lee, Y. E. Kwon, Y. J. Kim and J. S. Choi, *Macromole. Res.*, **27**(4), 360 (2019).
27. L. T. Thuy, S. Mallick and J. S. Choi, *Int. J. Pharm.*, **492**(1-2), 233 (2015).
28. A. M. Wade and H. N. Tucker, *J. Nutr. Biochem.*, **9**(6), 315 (1998).
29. A. Mecke, S. Uppuluri, T. M. Sassanella, D. K. Lee, A. Ramamoorthy, J. R. Baker Jr., G. O. Bradford and M. M. B. Holl, *Chem. Phys. Lipids*, **132**(1), 3 (2004).
30. A. J. Geall and I. S. Blagbrough, *J. Pharm. Biomed.*, **22**(5), 849 (2000).
31. H. Eliyahu, Y. Barenholz and A. Domb, *Molecules*, **10**(1), 34 (2005).
32. B. D. Monnery, *Biomacromolcules*, **22**(10), 4060 (2021).
33. T. Bus, A. Traeger and U. S. Schubert, *J. Mater. Chem. B*, **6**(43), 6904 (2018).
34. S. Brunner, T. Sauer, S. Carotta, M. Cotten, M. Saltik and E. Wagner, *Gene Ther.*, **7**(5), 401 (2000).
35. A. Pantos, I. Tsogas and C. M. Paleos, *Biochim. Biophys. Acta-Biomembr.*, **1778**(4), 811 (2008).
36. N. Sakai, T. Takeuchi, S. Futaki and S. Matile, *ChemBioChem*, **6**(1), 114 (2005).
37. H. Chang, J. Zhang, H. Wang, J. Lv and Y. Cheng, *Biomacromolcules*, **18**(8), 2371 (2017).
38. F. Wang, K. Hu and Y. Cheng, *Acta Biomater.*, **29**, 94 (2016).
39. I. Tsogas, D. Tsiourvas, G. Nounesis and C. M. Paleos, *Langmuir*, **22**(26), 11322 (2006).
40. J. S. Choi, K. Nam, J. Y. Park, J. B. Kim, J. K. Lee and J. S. Park, *J. Control. Release*, **99**(3), 445 (2004).
41. N. Panté and M. Kann, *J. Mol. Cell Biol.*, **13**(2), 425 (2002).
42. P. C. Naha, M. Davoren, F. M. Lyng and H. Byrne, *Toxicol. Appl. Pharmacol.*, **246**(1-2), 91 (2010).

Supporting Information

Low generational cystamine core PAMAM derivatives modified with nuclear localization signal derived from lactoferrin as a gene carrier

Jeil Lee*, Yong-Eun Kwon, Hwanuk Guim***, and Kyung Jae Jeong*,†**

*Department of Chemical Engineering, University of New Hampshire, Durham, New Hampshire 03824, United States
**Center for Scientific Instrumentation, Korea Basic Science Institute, 169-148 Gwahak-ro, Yuseong-gu, Daejeon 34133, Korea
***Research Center for Materials Analysis, Korea Basic Science Institute, 169-148 Gwahak-ro, Yuseong-gu, Daejeon 34133, Korea
(*Received 15 July 2022 • Revised 13 September 2022 • Accepted 15 September 2022*)

Table S1. Stepwise conjugation yield of the polymers calculated by ^{1}H NMR

	Gly	Arg	Arg	Arg	Arg	His	Final yield
GRRRRH-cPG0	>30%	>99%	>99%	>99%	>99%	>99%	>30%
GRRRRH-cPG1	>99%	>99%	>99%	>99%	>99%	>99%	>99%
GRRRRH-cPG2	>92%	>92%	>92%	>92%	>92%	>82%	>82%

Table S2. One-way analysis of variance (ANOVA) results of about transfection efficiency of each polymer in NIH3T3, MCF-7, HDF cells. It means that missing information has no significance statistically. *P<0.05, **P<0.01, and ***P<0.001

NIH3T3 cells

Tukey's Multiple Comparison Test	Mean Diff.	q	Significant P<0.05	Summary	95% CI of diff
PEI 25 kDa vs GRRRRH-cPG1 16:1	−811,700	15.65	Yes	***	−1,084,000 to −539,400
PEI 25 kDa vs GRRRRH-cPG2 12:1	−590,000	11.37	Yes	***	−862,300 to −317,700
PEI 25 kDa vs GRRRRH-cPG2 16:1	−1,161,000	22.39	Yes	***	−1,433,000 to −888,800
cPG2 vs GRRRRH-cPG1 16:1	−1,037,000	19.99	Yes	***	−1,309,000 to −764,700
cPG2 vs GRRRRH-cPG2 12:1	−815,300	15.72	Yes	***	−1,088,000 to −543,000
cPG2 vs GRRRRH-cPG2 16:1	−1,386,000	26.73	Yes	***	−1,659,000 to −1,114,000
cPG1 vs GRRRRH-cPG1 16:1	−1,041,000	20.06	Yes	***	−1,313,000 to −768,300
cPG1 vs GRRRRH-cPG2 12:1	−818,800	15.79	Yes	***	−1,091,000 to −546,600
cPG1 vs GRRRRH-cPG2 16:1	−1,390,000	26.8	Yes	***	−1,662,000 to −1,118,000
cPG0 vs GRRRRH-cPG1 16:1	−1,041,000	20.06	Yes	***	−1,313,000 to −768,300
cPG0 vs GRRRRH-cPG2 12:1	−818,800	15.79	Yes	***	−1,091,000 to −546,500
cPG0 vs GRRRRH-cPG2 16:1	−1,390,000	26.8	Yes	***	−1,662,000 to −1,118,000
GRRRRH-cPG0 4:1 vs GRRRRH-cPG1 16:1	−1,024,000	19.75	Yes	***	−1,297,000 to −752,100
GRRRRH-cPG0 4:1 vs RRRRH-cPG2 12:1	−802,700	15.48	Yes	***	−1,075,000 to −530,400
GRRRRH-cPG0 4:1 vs RRRRH-cPG2 16:1	−1,374,000	26.49	Yes	***	−1,646,000 to −1,102,000
GRRRRH-cPG0 8:1 vs GRRRRH-cPG1 16:1	−1,028,000	19.82	Yes	***	−1,300,000 to −755,500
GRRRRH-cPG0 8:1 vs GRRRRH-cPG2 12:1	−806,100	15.54	Yes	***	−1,078,000 to −533,800
GRRRRH-cPG0 8:1 vs GRRRRH-cPG2 16:1	−1,377,000	26.55	Yes	***	−1,649,000 to −1,105,000
GRRRRH-cPG0 12:1 vs GRRRRH-cPG1 16:1	−1,024,000	19.73	Yes	***	−1,296,000 to −751,300
GRRRRH-cPG0 12:1 vs GRRRRH-cPG2 12:1	−801,800	15.46	Yes	***	−1,074,000 to −529,500
GRRRRH-cPG0 12:1 vs GRRRRH-cPG2 16:1	−1,373,000	26.47	Yes	***	−1,645,000 to −1,101,000
GRRRRH-cPG0 16:1 vs GRRRRH-cPG1 16:1	−1,015,000	19.56	Yes	***	−1,287,000 to −742,200
GRRRRH-cPG0 16:1 vs GRRRRH-cPG2 12:1	−792,800	15.28	Yes	***	−1,065,000 to −520,500
GRRRRH-cPG0 16:1 vs GRRRRH-cPG2 16:1	−1,364,000	26.3	Yes	***	−1,636,000 to −1,092,000
GRRRRH-cPG1 4:1 vs GRRRRH-cPG1 16:1	−1,025,000	19.76	Yes	***	−1,297,000 to −752,900

GRRRRH-cPG1 4:1 vs GRRRRH-cPG2 12:1	−803,400	15.49	Yes	***	−1,076,000 to −531,100
GRRRRH-cPG1 4:1 vs GRRRRH-cPG2 16:1	−1,375,000	26.5	Yes	***	−1,647,000 to −1,102,000
GRRRRH-cPG1 8:1 vs GRRRRH-cPG1 16:1	−1,015,000	19.56	Yes	***	−1,287,000 to −742,300
GRRRRH-cPG1 8:1 vs GRRRRH-cPG2 12:1	−792,900	15.29	Yes	***	−1,065,000 to −520,600
GRRRRH-cPG1 8:1 vs GRRRRH-cPG2 16:1	−1,364,000	26.3	Yes	***	−1,636,000 to −1,092,000
GRRRRH-cPG1 12:1 vs GRRRRH-cPG1 16:1	−947,400	18.27	Yes	***	−1,220,000 to −675,100
GRRRRH-cPG1 12:1 vs GRRRRH-cPG2 12:1	−725,700	13.99	Yes	***	−997,900 to −453,400
GRRRRH-cPG1 12:1 vs GRRRRH-cPG2 16:1	−1,297,000	25	Yes	***	−1,569,000 to −1,025,000
GRRRRH-cPG1 16:1 vs GRRRRH-cPG2 4:1	1,021,000	19.68	Yes	***	748,500 to 1,293,000
GRRRRH-cPG1 16:1 vs GRRRRH-cPG2 8:1	895,000	17.26	Yes	***	622,700 to 1,167,000
GRRRRH-cPG1 16:1 vs GRRRRH-cPG2 16:1	−349,400	6.736	Yes	**	−621,700 to −77,130
GRRRRH-cPG2 4:1 vs GRRRRH-cPG2 12:1	−799,000	15.41	Yes	***	−1,071,000 to −526,800
GRRRRH-cPG2 4:1 vs GRRRRH-cPG2 16:1	−1,370,000	26.42	Yes	***	−1,642,000 to −1,098,000
GRRRRH-cPG2 8:1 vs GRRRRH-cPG2 12:1	−673,200	12.98	Yes	***	−945,500 to −401,000
GRRRRH-cPG2 8:1 vs GRRRRH-cPG2 16:1	−1,244,000	23.99	Yes	***	−1,517,000 to −972,100
GRRRRH-cPG2 12:1 vs GRRRRH-cPG2 16:1	−571,100	11.01	Yes	***	−843,400 to −298,900

MCF-7 cells

Tukey's Multiple Comparison Test	Mean Diff.	q	Significant P<0.05	Summary	95% CI of diff
PEI 25 kDa vs cPG2	2,823,000	7.556	Yes	***	861,700 to 4,784,000
PEI 25 kDa vs cPG1	2,874,000	7.693	Yes	***	912,800 to 4,835,000
PEI 25 kDa vs cPG0	2,870,000	7.683	Yes	***	909,100 to 4,832,000
PEI 25 kDa vs GRRRRH-cPG0 4:1	2,872,000	7.686	Yes	***	910,300 to 4,833,000
PEI 25 kDa vs GRRRRH-cPG0 8:1	2,777,000	7.432	Yes	***	815,500 to 4,738,000
PEI 25 kDa vs GRRRRH-cPG0 12:1	2,617,000	7.004	Yes	**	655,700 to 4,578,000
PEI 25 kDa vs GRRRRH-cPG0 16:1	2,272,000	6.082	Yes	*	311,200 to 4,234,000
PEI 25 kDa vs GRRRRH-cPG1 4:1	2,664,000	7.132	Yes	**	703,200 to 4,626,000
PEI 25 kDa vs GRRRRH-cPG1 8:1	2,168,000	5.803	Yes	*	206,900 to 4,129,000
PEI 25 kDa vs GRRRRH-cPG1 12:1	2,426,000	6.494	Yes	**	465,100 to 4,388,000
PEI 25 kDa vs GRRRRH-cPG1 16:1	1,998,000	5.347	Yes	*	36,400 to 3,959,000
PEI 25 kDa vs GRRRRH-cPG2 4:1	2,292,000	6.136	Yes	*	331,200 to 4,254,000
cPG2 vs GRRRRH-cPG2 12:1	−3,264,000	8.738	Yes	***	−5,226,000 to −1,303,000
cPG2 vs GRRRRH-cPG2 16:1	−4,780,000	12.79	Yes	***	−6,741,000 to −2,819,000
cPG1 vs GRRRRH-cPG2 8:1	−1,983,000	5.307	Yes	*	−3,944,000 to −21,470
cPG1 vs GRRRRH-cPG2 12:1	−3,316,000	8.874	Yes	***	−5,277,000 to −1,354,000
cPG1 vs GRRRRH-cPG2 16:1	−4,831,000	12.93	Yes	***	−6,792,000 to −2,870,000
cPG0 vs GRRRRH-cPG2 8:1	−1,979,000	5.297	Yes	*	−3,940,000 to −17,800
cPG0 vs GRRRRH-cPG2 12:1	−3,312,000	8.865	Yes	***	−5,273,000 to −1,351,000
cPG0 vs GRRRRH-cPG2 16:1	−4,828,000	12.92	Yes	***	−6,789,000 to −2,866,000
GRRRRH-cPG0 4:1 vs GRRRRH-cPG2 8:1	−1,980,000	5.3	Yes	*	−3,941,000 to −18,980
GRRRRH-cPG0 4:1 vs GRRRRH-cPG2 12:1	−3,313,000	8.868	Yes	***	−5,274,000 to −1,352,000
GRRRRH-cPG0 4:1 vs GRRRRH-cPG2 16:1	−4,829,000	12.92	Yes	***	−6,790,000 to −2,868,000
GRRRRH-cPG0 8:1 vs GRRRRH-cPG2 12:1	−3,218,000	8.614	Yes	***	−5,179,000 to −1,257,000
GRRRRH-cPG0 8:1 vs GRRRRH-cPG2 16:1	−4,734,000	12.67	Yes	***	−6,695,000 to −2,773,000
GRRRRH-cPG0 12:1 vs GRRRRH-cPG2 12:1	−3,058,000	8.186	Yes	***	−5,020,000 to −1,097,000
GRRRRH-cPG0 12:1 vs GRRRRH-cPG2 16:1	−4,574,000	12.24	Yes	***	−6,535,000 to −2613000
GRRRRH-cPG0 16:1 vs GRRRRH-cPG2 12:1	−2,714,000	7.264	Yes	**	−4,675,000 to −752,700
GRRRRH-cPG0 16:1 vs GRRRRH-cPG2 16:1	−4,230,000	11.32	Yes	***	−6,191,000 to −2,268,000
GRRRRH-cPG1 4:1 vs GRRRRH-cPG2 12:1	−3,106,000	8.313	Yes	***	−5,067,000 to −1,145,000
GRRRRH-cPG1 4:1 vs GRRRRH-cPG2 16:1	−4,622,000	12.37	Yes	***	−6,583,000 to −2,660,000
GRRRRH-cPG1 8:1 vs GRRRRH-cPG2 12:1	−2,610,000	6.985	Yes	**	−4,571,000 to −648,500
GRRRRH-cPG1 8:1 vs GRRRRH-cPG2 16:1	−4,125,000	11.04	Yes	***	−6,087,000 to −2,164,000

GRRRRH-cPG1 12:1 vs GRRRRH-cPG2 12:1	−2,868,000	7.676	Yes	***	−4,829,000 to −906,700
GRRRRH-cPG1 12:1 vs GRRRRH-cPG2 16:1	−4,384,000	11.73	Yes	***	−6,345,000 to −2,422,000
GRRRRH-cPG1 16:1 vs GRRRRH-cPG2 12:1	−2,439,000	6.529	Yes	**	−4,400,000 to −478,000
GRRRRH-cPG1 16:1 vs GRRRRH-cPG2 16:1	−3,955,000	10.59	Yes	***	−5,916,000 to −1,994,000
GRRRRH-cPG2 4:1 vs GRRRRH-cPG2 12:1	−2,734,000	7.318	Yes	**	−4,695,000 to −772,700
GRRRRH-cPG2 4:1 vs GRRRRH-cPG2 16:1	−4,250,000	11.37	Yes	***	−6,211,000 to −2,288,000
GRRRRH-cPG2 8:1 vs GRRRRH-cPG2 16:1	−2,849,000	7.624	Yes	***	−4,810,000 to −887,300

HDF cells

Tukey's Multiple Comparison Test	Mean Diff.	q	Significant P<0.05	Summary	95% CI of diff
PEI 25 kDa vs cPG0	1,157,000	8.778	Yes	***	465,000 to 1,849,000
PEI 25 kDa vs cPG1	1,158,000	8.788	Yes	***	466,400 to 1,850,000
PEI 25 kDa vs cPG2	1,158,000	8.783	Yes	***	465,800 to 1,850,000
PEI 25 kDa vs GRRRRH-cPG0 4:1	1,156,000	8.772	Yes	***	464,400 to 1,848,000
PEI 25 kDa vs GRRRRH-cPG0 8:1	1,121,000	8.506	Yes	***	429,300 to 1,813,000
PEI 25 kDa vs GRRRRH-cPG0 12:1	1,127,000	8.55	Yes	***	435,100 to 1,819,000
PEI 25 kDa vs GRRRRH-cPG0 16:1	1,100,000	8.347	Yes	***	408,300 to 1,792,000
PEI 25 kDa vs GRRRRH-cPG1 4:1	958,800	7.274	Yes	**	266,900 to 1,651,000
PEI 25 kDa vs GRRRRH-cPG1 8:1	874,000	6.63	Yes	**	182,000 to 1,566,000
PEI 25 kDa vs GRRRRH-cPG1 12:1	747,100	5.668	Yes	*	55,130 to 1,439,000
PEI 25 kDa vs GRRRRH-cPG1 16:1	770,000	5.842	Yes	*	78,050 to 1,462,000
PEI 25 kDa vs GRRRRH-cPG2 4:1	914,100	6.935	Yes	**	222,100 to 1,606,000
cPG0 vs GRRRRH-cPG2 8:1	−780,400	5.921	Yes	*	−1,472,000 to −88,500
cPG0 vs GRRRRH-cPG2 12:1	−1,336,000	10.14	Yes	***	−2,028,000 to −644,500
cPG0 vs GRRRRH-cPG2 16:1	−696,600	5.285	Yes	*	−1,388,000 to −4,640
cPG1 vs GRRRRH-cPG2 8:1	−781,800	5.931	Yes	*	−1,474,000 to −89,880
cPG1 vs GRRRRH-cPG2 12:1	−1,338,000	10.15	Yes	***	−2,030,000 to −645,800
cPG1 vs GRRRRH-cPG2 16:1	−698,000	5.295	Yes	*	−1,390,000 to −6,024
cPG2 vs GRRRRH-cPG2 8:1	−781,200	5.927	Yes	*	−1,473,000 to −89,270
cPG2 vs GRRRRH-cPG2 12:1	−1,337,000	10.14	Yes	***	−2,029,000 to −645,200
cPG2 vs GRRRRH-cPG2 16:1	−697,300	5.29	Yes	*	−1,389,000 to −5,414
GRRRRH-cPG0 4:1 vs GRRRRH-cPG2 8:1	−779,700	5.916	Yes	*	−1,472,000 to −87,800
GRRRRH-cPG0 4:1 vs GRRRRH-cPG2 12:1	−1,336,000	10.13	Yes	***	−2,028,000 to −643,800
GRRRRH-cPG0 4:1 vs GRRRRH-cPG2 16:1	−695,900	5.279	Yes	*	−1,388,000 to −3,941
GRRRRH-cPG0 8:1 vs GRRRRH-cPG2 8:1	−744,700	5.65	Yes	*	−1,437,000 to −52,760
GRRRRH-cPG0 8:1 vs GRRRRH-cPG2 12:1	−1,301,000	9.867	Yes	***	−1,993,000 to −608,700
GRRRRH-cPG0 12:1 vs GRRRRH-cPG2 8:1	−750,500	5.694	Yes	*	−1,442,000 to −58,560
GRRRRH-cPG0 12:1 vs GRRRRH-cPG2 12:1	−1,306,000	9.912	Yes	***	−1,998,000 to −614,500
GRRRRH-cPG0 16:1 vs GRRRRH-cPG2 8:1	−723,700	5.49	Yes	*	−1,416,000 to −31,780
GRRRRH-cPG0 16:1 vs GRRRRH-cPG2 12:1	−1,280,000	9.708	Yes	***	−1,972,000 to −587,700
GRRRRH-cPG1 4:1 vs GRRRRH-cPG2 12:1	−1,138,000	8.635	Yes	***	−1,830,000 to −446,300
GRRRRH-cPG1 8:1 vs GRRRRH-cPG2 12:1	−1,053,000	7.992	Yes	***	−1,745,000 to −361,400
GRRRRH-cPG1 12:1 vs GRRRRH-cPG2 12:1	−926,500	7.029	Yes	**	−1,618,000 to −234,500
GRRRRH-cPG1 16:1 vs GRRRRH-cPG2 12:1	−949,400	7.203	Yes	**	−1,641,000 to −257,500
GRRRRH-cPG2 4:1 vs GRRRRH-cPG2 12:1	-1,093,000	8.296	Yes	***	−1,785,000 to −401,500

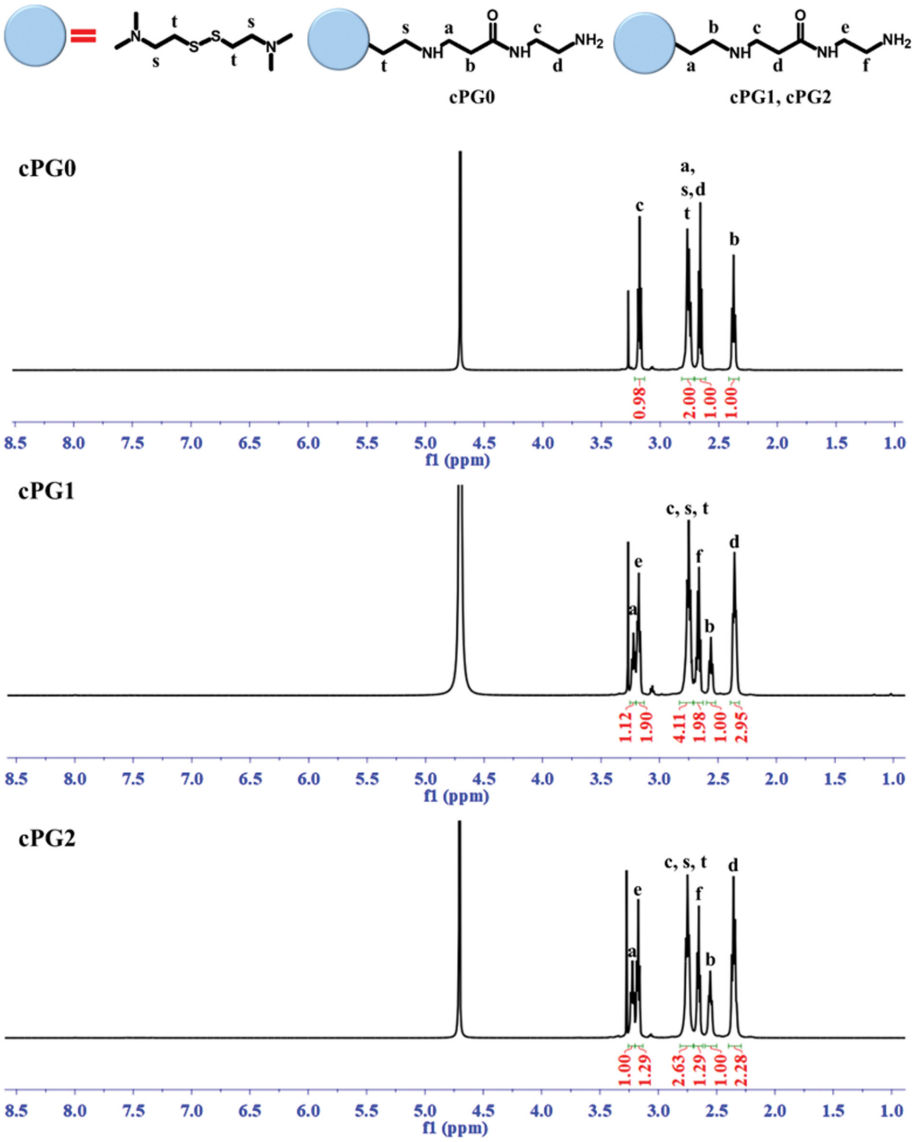

Fig. S1. ^{1}**H NMR spectra of cPAMAM.**

cPG0: δ (in ppm) 2.37 (-$NCH_2C\mathbf{H}_2CO$- of cPAMAM), 2.66 (-$CONHCH_2C\mathbf{H}_2NH_2$ of cPAMAM), 2.77 (-$NC\mathbf{H}_2CH_2CO$- of cPAMAM, -$SC\mathbf{H}_2CH_2N$- of cPAMAM, -$SCH_2C\mathbf{H}_2N$- of cPAMAM), 3.18 (-$CONHC\mathbf{H}_2CH_2NH_2$ of cPAMAM).

cPG1: δ (in ppm) 2.36 (-$NCH_2C\mathbf{H}_2CO$- of cPAMAM), 2.56 (-$CONHCH_2C\mathbf{H}_2N$- of cPAMAM), 2.66 (-$CONHCH_2C\mathbf{H}_2NH_2$ of cPAMAM), 2.75 (-$NC\mathbf{H}_2CH_2CO$- of PAMAM, -$SC\mathbf{H}_2CH_2N$- of cPAMAM, and -$SCH_2C\mathbf{H}_2N$- of cPAMAM) 3.18 (-$CONHC\mathbf{H}_2CH_2N$- of cPAMAM), and 3.22 (-$CONHC\mathbf{H}_2CH_2NH_2$ of cPAMAM).

cPG2: δ (in ppm) 2.36 (-$NCH_2C\mathbf{H}_2CO$- of cPAMAM), 2.55 (-$CONHCH_2C\mathbf{H}_2N$- of cPAMAM), 2.65 (-$CONHCH_2C\mathbf{H}_2NH_2$ of cPAMAM), 2.75 (-$NC\mathbf{H}_2CH_2CO$- of PAMAM, -$SC\mathbf{H}_2CH_2N$- of cPAMAM, and -$SCH_2C\mathbf{H}_2N$- of cPAMAM) 3.17(-$CONHC\mathbf{H}_2CH_2N$- of cPAMAM), and 3.22 (-$CONHC\mathbf{H}_2CH_2NH_2$ of cPAMAM).

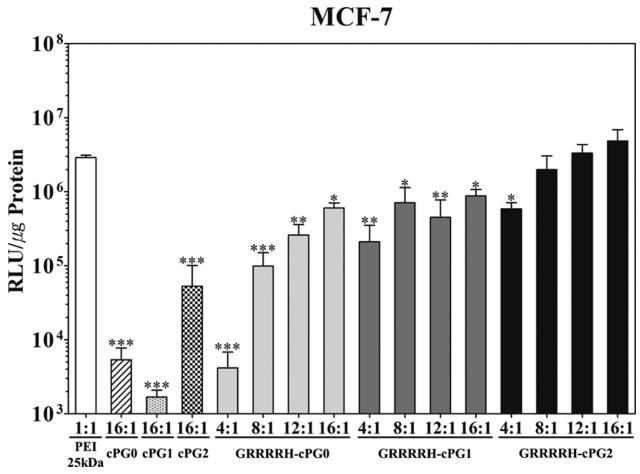

Fig. S2. Transfection efficiency of cPAMAM derivatives in MCF-7 cells. Data are shown as mean±standard deviation (n=3).

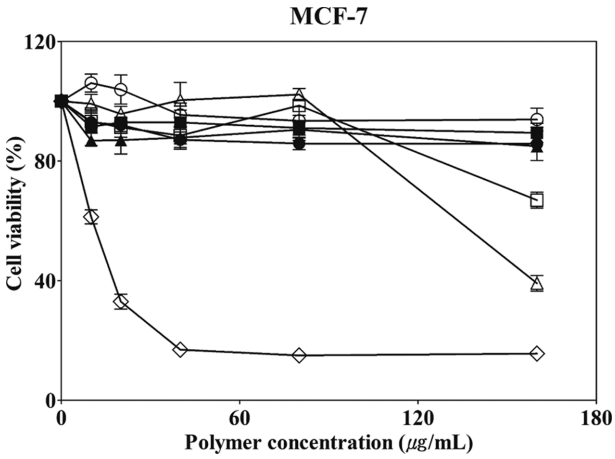

Fig. S3. Cytotoxicity assay in MCF-7 cells using Alarmar assay. PEI 25 kDa (◇), cPG0 (●), cPG1 (■), cPG2 (▲), GRRRRH-cPG0 (○), GRRRRH-cPG1 (□), GRRRRH-cPG2 (△). Data are shown as mean±standard deviation (n=3).

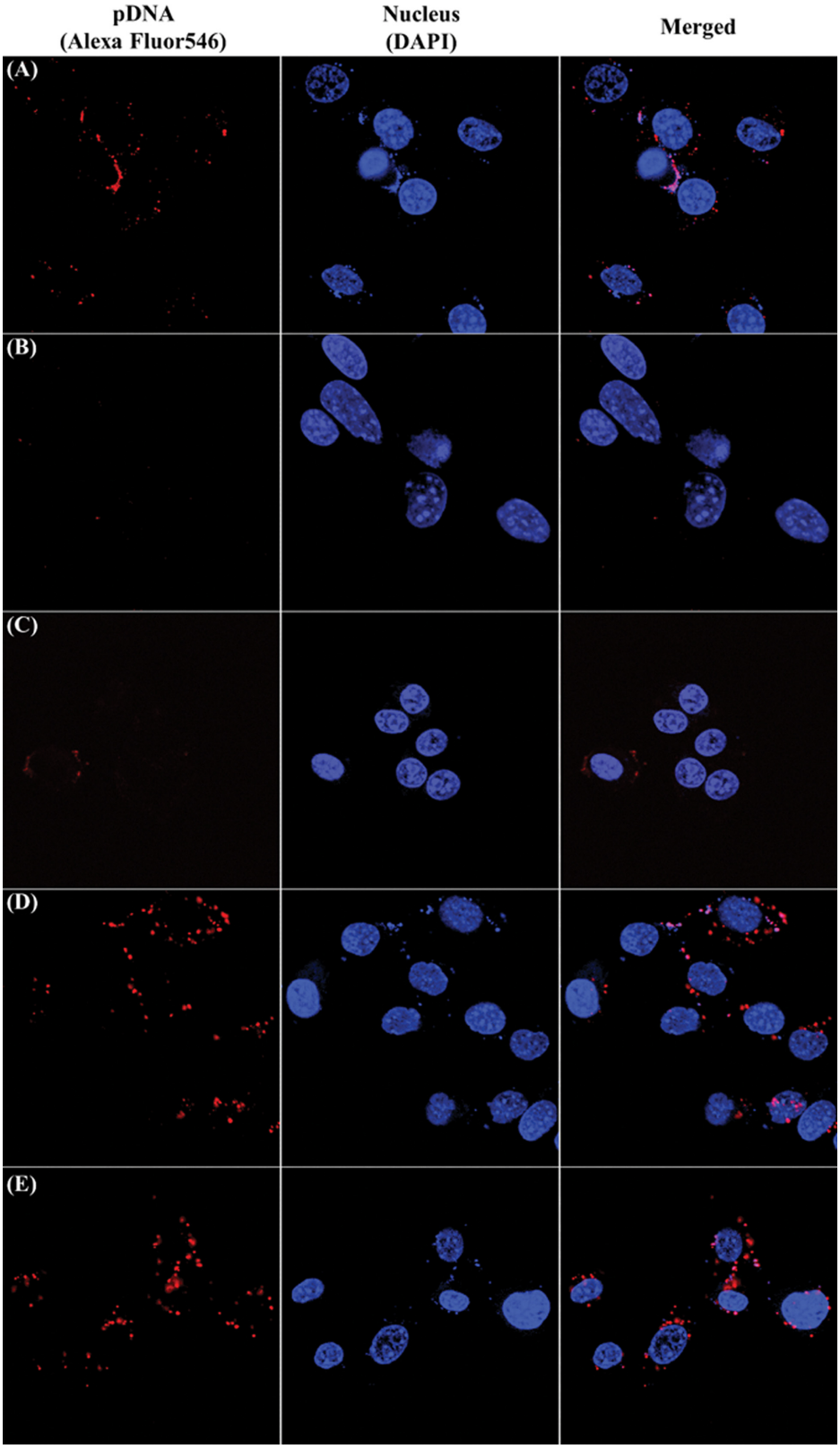

Fig. S4. Confocal microscopy images of polyplexes of (a) PEI 25 kDa, (b) cPG0, (c) cPG1, (d) GRRRRH-cPG0, (e) GRRRRH-cPG1 with pCN-Luci in NIH3T3 cells.